

A Novel Small Molecule Regulator of Guanine Nucleotide Exchange Activity of ARF and Golgi Membrane Trafficking*

8/11/2008

Heling Pan¹, Jia Yu¹, Lihong Zhang¹, Anne Carpenter², Hong Zhu³, Li Li¹, Dawei Ma^{1,4} and Junying Yuan^{3,4}.

¹State Key Laboratory of Bio-organic & Natural Products Chemistry, Shanghai Institute of Organic Chemistry, Chinese Academy of Sciences, 354 Fenglin Road, Shanghai 200032, China; ²Broad Institute of Harvard and MIT, 7 Cambridge Center, Cambridge, MA 02142; ³Department of Cell Biology, Harvard Medical School, 240 Longwood Ave, Boston, MA 02115, USA;

⁴Corresponding authors: jyuan@hms.harvard.edu, madw@pub.sioc.ac.cn

An image-based phenotypic screen was developed to identify small molecule regulators of intracellular traffic. Using this screen we found that AG1478, a previous known inhibitor of epidermal growth factor receptor (EGFR), had an EGFR independent activity in inducing the disassembly of the Golgi in human cells. Similar to Brefeldin A (BFA), a known disrupter of the Golgi, AG1478 inhibits the activity of small GTPase ARF. Unlike BFA, AG1478 exhibits low cytotoxicity and selectively targets the *cis*-Golgi without affecting endosomal compartment. We show that AG1478 inhibits GBF1, a large nucleotide exchange factor for ARF, in a Sec7 domain dependent manner and mimics the phenotype of a GBF1 mutant that has an inactive mutation. The treatment with AG1478 leads to the recruitment of GBF1 to the VTCs adjacent to the ERES, a step only transiently observed previously in the presence of BFA. We propose that the treatment with AG1478 delineates a membrane trafficking intermediate step that depends upon the Sec7 domain.

The Golgi apparatus, an intracellular membrane-bound structure organized as a series of

stacked cisternae and tubules, plays an important role in packaging and transporting macromolecules. The cisternae stack can be divided into five functional regions: the *cis*-Golgi network, *cis*-Golgi, medial-Golgi, trans-Golgi, and trans-Golgi network. Newly synthesized proteins and lipids are delivered by the coat protein complex II (COPII) vesicles from the endoplasmic reticulum (ER) via the vesicular-tubular clusters (VTCs) to the *cis*-Golgi network and subsequently progress through the stack to the trans-Golgi network, where they are packaged and sent to the cell surface, secretory vesicles or late endosomal compartments (1,2). p58 (also called ERGIC53), a cargo receptor involved in transporting proteins from the endoplasmic reticulum (ER) to the Golgi complex, has been used as a marker for the vesicular tubular clusters structure (VTCs) and the *cis*-Golgi (3,4).

The integrity and functions of the Golgi depend critically on the small membrane-bound vesicles that shuttle macromolecules in and out of the Golgi stacks (5). The ADP-ribosylation factor (ARF), a small GTPase of the Ras superfamily, plays a major role in driving Golgi membrane trafficking by recruiting coatomer (COPI) to Golgi membranes in the exocytotic pathway. The cellular

activity of ARFs is stimulated by the Sec7 family of guanine nucleotide exchange factors (GEFs) which promote the exchange of inactive GDP-bound to active GTP-bound forms (6,7). GBF1, the only known GEF localized to the *cis*-Golgi, plays an important role in mediating protein trafficking between the ER and the *cis*-Golgi (8,9).

Brefeldin A (BFA), a lactone isolated from fungi, interferes with anterograde transport from the endoplasmic reticulum to the Golgi apparatus by binding to the ARF1-GDP-Sec7 complex to inhibit the Sec7 guanine nucleotide exchange activity which in turn prevents the activation of ARF (10,11). The treatment with BFA causes rapid but reversible dispersal of the Golgi apparatus leading to the mixing of the *cis*-Golgi with the ER and vesicularization of the *trans*-Golgi network (12,13). BFA has pleiotropic effects on intracellular organelles other than the Golgi. For example, BFA induces extensive formation of membrane tubules from endosome compartment (14-16). BFA is highly cytotoxic and causes rapid cell death. It is not clear if its toxicity is related to its effects on Golgi dispersal (13,17,18).

In an effort to discover novel small molecules as tools to study membrane trafficking, we developed an image-based assay for compounds that can induce disassembly of the Golgi. In this manuscript, we show that tyrphostin AG1478 inhibits the nucleotide exchange of ARF1 in a manner dependent upon the Sec7 domain of GBF1.

Experimental Procedures

Plasmids, Antibodies and Cell Reagents

—AG1478, BFA, Nocodazole, Bafilomycin A1, EGF, H89 and 2-deoxy-D-glucose were from Sigma-Aldrich. The EGFR inhibitors were from ICCB Known Bioactives Library. AIFx was

prepared by (50 μ M AlCl₃ + 30 mM NaF) before use (19). Polyclonal rabbit anti-sec13 antibody was a kind gift from Wanjin Hong (Institute Molecular Biology, Singapore). Monoclonal anti-GM130, anti-GBF1, anti-p230, anti-Adaptin γ and anti-Adaptin δ antibodies were purchased from BD Biosciences. Monoclonal anti- α tubulin, anti-myc and polyclonal rabbit anti-calnexin antibodies were from Sigma-Aldrich. Monoclonal anti-phospho-EGFR, monoclonal anti-phospho-ERK and polyclonal rabbit anti-EGFR antibodies were from Cell Signaling Technology. Alexa Fluor 546 conjugated transferrin and LysoTracker red DND-99 were purchased from Molecular Probes. Polyclonal rabbit anti-GFP antibody and monoclonal anti-LAMP3 was from Santa Cruz Biotechnology. Polyclonal rabbit anti- β -COP antibody was from Affinity Bioreagents. Secondary antibodies conjugated with Texas Red or FITC were from Rockland Immunochemicals.

p58-YFP, GalT-CFP and ARF1-GFP were kind gifts from Jennifer Lippincott-Schwartz (National Institutes of Health, Bethesda). GBF1-GFP and E794K-GFP were kindly provided by Elizabeth Sztul (University of Alabama, Birmingham). Sec13-GFP, ERGIC53-myc and GST-VHS-GAT-GGA₃ were kind gifts from Benjamin S. Glick (University of Chicago, Chicago), Hans-Peter Hauri (University of Basel, Basel) and Paul A. Randazzo (National Institutes of Health, Bethesda). The different deleted constructs of GBF1-1 or GBF1-2 were digested from GBF1-GFP. The constructs were verified by sequencing.

Cell culture and transfection—Cells used for the experiments were maintained in Dulbecco's modified Eagle's medium supplemented with 10% fetal bovine serum, 100 units/ml penicillin/streptomycin, and 2 mM L-glutamine (Invitrogen) at 37°C, 5% CO₂. Transfection of H4 cells was

done using Lipofectamine 2000 reagent (Invitrogen). Stable cell line expressing p58-YFP was established in the presence of 1mg/ml G418 (Invitrogen).

Phenotypic screen—H4-p58 cells were plated in 96 well-plates at 3,000 cells per 100 μ l per well and cultured in a 5% CO₂ incubator overnight. Compounds were diluted by sampling 100 μ l of 5mg/ml or 0.5mg/ml of stocks dissolved in DMSO from the ICCB Known Bioactives Library of 480 compounds and transferred into wells in duplication. The images were visually examined using fluorescence microscopy (IX81, Olympus) after incubating with the compounds for 4 h, 8 h and 24 h. DMSO (0.1%) and BFA (5 μ M) were used as negative or positive control, respectively.

Immunofluorescence Microscopy and image analysis—Cells grown on coverslips were prepared and washed with PBS for three times, fixed in 3.8% paraformaldehyde (Sigma) for 20 min at room temperature. After blocked with 1% BSA in TBST for 30 min, cells were incubated with primary antibody diluted in 1% BSA /TBST for 2h or over night at 4°C. Coverslips were washed with TBST for three times and incubated with secondary antibody diluted in 1% BSA /TBST for 1h at room temperature. Coverslips were washed with TBST for three times again, stained with 4,6-diamidino-2-phenylindole (DAPI; 1 μ g/ml; Sigma) and mounted on slides with Fluorescent Mounting Medium (DAKO). Cells were imaged using a fluorescent microscopy (IX81, Olympus) with a 100 \times oil 1.35 NA objective and Image-Pro Express software (Media Cybernetics). Confocal images (Figure 8) were acquired using an LSM 510 (Carl Zeiss) with a 100 \times oil 1.35 NA objective and a single focal plane (0.9 μ m) was analyzed. For Figure 1, the analysis for Golgi dispersal course was performed using CellProfiler software. The analysis pipeline used to quantify images by CellProfiler was, briefly,

as follows: after correcting the illumination pattern across the field of view for each channel, nuclei were identified based on the DNA-stained images. Then, a ring 36 pixels around each nucleus was defined as a proxy for the cytoplasm. Within each cell, the Golgi were identified based on the GM130-stained image. Over 300 features were measured for each cell in each image; the most reliable measure of the change in Golgi localization was found to be a texture measure of the GM130 staining within each cell (Sum Average, at a scale of 5, nucleus + cytoplasm together). Example processed images are shown in *Supplementary Fig. 3*

EGFR siRNA—For transient inhibition of EGFR mRNA production, the small interfering RNA (siRNA) targeting the EGFR was synthesized (20): 5'-CTCTGGAGGAAAAGAAAGT-3' and 5'-ACTTTCTTTTCTCCAGAG-3'. H4 cells were co-transfected EGFR siRNA or negative control siRNA with pEGFP-N1 plasmid at 10:1 ratio by Lipofectamine 2000 reagent (Invitrogen). After 24h, cells were treated with compounds and analysed by western blotting for EGFR siRNA effect. The experiments were repeated twice with consistent results.

ARF1-GTP Pull Down Assay—The pull down assay to assess the activity of ARF1 by a GST-VHS-GAT-GGA₃ protein were performed as described previously (21,22). The stable H4-ARF1-GFP cells were transiently transfected with GBF1-GFP for 24h or pEGFP-C1 or vector alone, then treated with compounds. Cells were lysed with pull down buffer (50 mM Tris-HCl, pH 7.5, 100 mM NaCl, 2 mM MgCl₂, 1% Triton X-100, and protease inhibitors). Cell lysates were cleared by glutathione-Sepharose beads and incubated with beads containing fifty μ g GST-VHS-GAT-GGA₃ protein for 2 h at 4°C. The bound proteins were removed and analyzed by western blotting using anti-GFP antibody.

Cell fractionation—The cell fractionation assay was performed as described previously (23). H4 cells were grown on 100 cm dishes for 24h and treated with compounds. Cells were washed with PBS and lysed with ice-cold homogenization buffer (50 mM HEPES, pH 7.5, 100 mM KCl, 1 mM MgCl₂, 1mM DTT and protease inhibitors) by passing ten times through a 22G needle and centrifuged at 1,000 g for 15 min at 4°C to remove unbroken cells. The postnuclear supernatant was centrifuged at 100,000 g for 60 min at 4°C to obtain cytosol and membrane fraction. The supernatant was used as cytosol fraction. The pellet was rinsed with homogenization buffer, dissolved in RIPA buffer and used as membrane fraction. Fractions containing same volume were analyzed by 6% SDS-PAGE and transferred to NC membrane. The membrane was detected by anti-GBF1, anti-calnexin and anti-tubulin antibodies respectively. Calnexin and tubulin were consider as standards for membrane and cytosol fraction.

RESULTS

An Image-Based Phenotypic Screen for Small Molecules that Disrupt the Golgi—We established a H4 human glioblastoma cell line stably expressing a p58-YFP fusion protein (H4-p58-YFP). p58-YFP normally appears in peripheral punctate structures close to the *cis*-Golgi (Fig 1A). Using H4-p58-YFP cells, we developed an image-based assay using fluorescent microscopy and screened the ICCB Known Bioactive Library for compounds that may have effects on Golgi morphology (Biomol catalogue #2840; www.biomol.com). H4-p58-YFP cells were plated in 96-well plates for 24 h and treated with different compounds individually at concentration of 3~12 μ M. 0.1% DMSO was used as a negative control. After incubating with the

compounds for 4 h, 8 h and 24 h, the images were visually examined using fluorescence microscopy. The screen was carried out in duplicates. Most of the compounds were found to have no effect on Golgi morphology. Twenty compounds were isolated as Golgi-disrupting agents. These include some well-known Golgi disrupting reagents such as brefeldin A, bafilomycin A1 and monensin (data not shown). Here we focus on tyrphostin AG1478, the most potent novel Golgi dispersing compound identified from our screen. It has a structure distinct from that of BFA (Fig. 1B).

AG1478 is a potent and reversible disruptor of the Golgi—The treatment of H4 cells with AG1478 caused p58-YFP to redistribute from its normal perinuclear compact localization to a dispersed localization throughout the cytosol in a manner very similar to that of BFA (Fig. 1A). The Golgi dispersing effect of AG1478 in the parental H4 cells which do not express p58-YFP was confirmed by indirect immunofluorescence using an antibody against GM130, a Golgi matrix protein (24). GM130 was redistributed to peripheral punctate structures throughout the cytoplasm after the treatment of AG1478 (Fig. 1C). We quantified the Golgi dispersing effect of AG1478 using the image analysis software, CellProfiler (25,26). We found that AG1478 can rapidly disperse the *cis*-Golgi protein GM130 with half-time of ~10 min and an EC₅₀ of 3.35 μ M (Fig. 1D and 1E). The effect of AG1478 on the Golgi was fully reversible as the normal Golgi structure reappeared in the perinuclear area after the cells were cultured in media without AG1478 for 3 hrs (Fig. 1F).

Unlike nocodazole or bafilomycin A1, which disperse the Golgi through their effects on the microtubules and intracellular pH, AG1478 had no apparent effect on the cytoskeleton or intracellular pH. The treatment of AG1478 for 1 hr also did not have any obvious effect on the intracellular ATP

levels (*supplemental Fig.1*). Furthermore, the ability of AG1478 to disrupt the Golgi was not associated with significant cytotoxicity: incubation of H4 cells in the presence of 14 μM AG1478 for 24 h had no detectable effect on cell survival. After 48 h, a loss of 25% of viability was observed which could be rescued by a caspase inhibitor zVAD.fmk. In contrast, the treatment of H4 cells with 5 μM BFA for 24 or 48 h led to significant loss of cell viability which could not be blocked by zVAD.fmk (*supplemental Fig.2*). From these results, we conclude that dispersing Golgi per se is not affecting the viability of H4 cells. Therefore, the cytotoxicity of BFA may not be directly linked to its ability to disrupt the Golgi.

The Effect of AG1478 on the Golgi Is Independent of EGFR—AG1478 was shown to be a highly potent inhibitor of the epidermal growth factor (EGF) receptor tyrosine kinase (27,28). Indeed, the treatment of H4 cells with 250 nM AG1478 was sufficient to block EGFR phosphorylation which is much lower than that of the EC_{50} required to disperse the Golgi (Fig. 2A). To further determine if the Golgi dispersing effect of AG1478 was associated with its inhibitory activity for EGFR, we treated H4 cells with multiple different EGFR inhibitors individually (AG213, Lavendustin A, and RG-14620), inhibitors for other RTPKs (AG-370, AG-879, and AG-825), as well as genistein which is a general inhibitor of tyrosine protein kinase. None of these inhibitors demonstrated a similar Golgi dispersing effect even at very high concentrations (50-100 μM) and after prolonged treatment time (2-4 hrs) (data not show). Thus, the Golgi dispersing ability of AG1478 is not shared by the other known tyrosine kinase inhibitors tested.

To formally exclude the involvement of EGFR, we used small interfering RNA (siRNA) to decrease the expression of EGFR. Expression of EGFR siRNAs for 24 hrs significantly decreased

the cellular levels of EGFR (Fig. 2B), but reducing the expression of EGFR had no effect on the Golgi structure per se, or the Golgi dispersing effect of AG1478 (Fig. 2C-F). From these results, we conclude that AG1478 has a distinct activity in inducing Golgi dispersing that is independent from its activity towards EGFR.

Rodent Cells Are Resistant to the Golgi dispersal by AG1478 But Not BFA—To characterize the Golgi dispersing effect of AG1478, we examined whether the Golgi structures in multiple cell lines are sensitive to AG1478. AG1478 showed a similar Golgi dispersing effect in different human cell lines tested, including HeLa, HepG2, A549 and Hs-578Bst fibroblast cells (*supplemental Table 1*). Surprisingly, AG1478 could not disrupt the Golgi structures in multiple rodent cell lines tested, including two rat cell lines, Rat2 and NRK, and a mouse cell line, NIH3T3. The Golgi complex marked by anti-GM130 antibody in Rat2 cells remained intact even after the treatment with AG1478 at concentrations as high as 140 μM (50 $\mu\text{g/ml}$) prolonged incubation (Fig. 3A). In contrast, Rat2 cells were fully sensitive to the Golgi dispersing effect of BFA (Fig. 3A).

To further ascertain the resistance of rodent cell lines to AG1478, we evaluated other markers of Golgi such as GalT, ERGIC53/p58, ARF1, $\beta\text{-COP}$ and GBF1 in AG1478 treated Rat2 cells. None of these proteins was redistributed from its normal perinuclear compact localization (data not shown). We also examined the effect of AG1478 in PtK1 and MDCK cells, which were kangaroo rat and dog epithelial cell lines, respectively, and reported to be resistant to BFA (29,30). The MDCK and PtK1 cells were also resistant to the effect of AG1478 in dispersing the Golgi. On the other hand, AG1478 inhibited the EGFR signaling pathway in both human and rodent cells (Fig. 3B), supporting the conclusion that the effect of

AG1478 for dispersing the Golgi is independent of its activity on EGFR. Taken together, these results suggest that AG1478 targets a molecular entity that exhibits species specificity for its Golgi dispersing effect.

Differential effects of AG1478 on the proteins associated the cis-Golgi and trans-Golgi—To understand the mechanism by which AG1478 disperses the Golgi, we compared the activity of AG1478 with that of BFA for their effects on the distribution of Golgi associated proteins. COPI has been shown to be the most important coat protein in facilitating retrograde intracellular transport from the Golgi complex to the ER. Recruitment of COPI to the membrane requires the activation of ARF1 (31,32). In control cells, most of COPI and ARF1 are localized on the *cis*-Golgi membrane. The addition of AG1478 caused a rapid release of COPI and ARF1 into the cytoplasm (Fig. 4A and B). The treatment with AG1478 also resulted in the redistribution of GBF1 from the Golgi region to a dispersed localization throughout the cytoplasm (Fig. 4C), an effect similar to that of BFA (33).

Sec13 is a component of the COPII coat that mediates vesicle budding from ER exit site (ERES) (34,35). The treatment with AG1478 had no effect on the distribution of Sec13-GFP, which is localized to the punctate ERES, suggesting that the treatment of AG1478 does not perturb the COP II -dependent ER export machinery (Fig. 4D). The treatment with AG1478, however, caused the redistribution of p58/ERGIC53, a marker for the VTCs, from its normal compact localization to a dispersed cytoplasmic localization (Fig. 4E). GM130, a Golgi matrix protein, was also redistributed to the peripheral punctate structures after treatment by AG1478, similar to that of BFA (Fig. 4F). The peripheral punctate structures of p58/ERGIC53 and GM130 were similar to the “Golgi remnants” after BFA treatment (36,37).

Galactosyltransferase (GalT), a Golgi resident enzyme, was found in both the ER and some punctate structures after the treatment with AG1478 (Fig. 4G). Taken together, the effects of AG1478 on the proteins localized in the *cis*-Golgi are very similar to that of BFA.

We also compared the effects of AG1478 and BFA on proteins associated with the *trans*-Golgi. After incubation of H4 cells with either compound for 1 h, 5 μ M BFA completely dispersed the *trans*-Golgi network marker p230 from the perinuclear region into the cytosol, whereas after AG1478 treatment p230 remained as small punctate structures with partial redistribution to the cytoplasm (Fig. 4H) (38). Longer treatment with AG1478 (2-3 hr) still did not completely disperse the punctate structures (data not shown). The effects of AG1478 on Adaptin γ and Adaptin δ , which are markers for AP-1 and AP-2, were similar to that of p230 (Fig. 4I and 4J). Taken together, these results suggest that the *cis*-Golgi is more sensitive to AG1478 than the *trans*-Golgi.

The treatment of BFA is known to cause extensive formation of membrane tubules from endosomes (15,39). Using Alexa 568-labeled transferrin we analyzed the effect of AG1478 on the formation of tubular endosomes. BFA induced enlargement and tubulation of transferrin-positive endosomes but AG1478 had no effect (Fig. 4K), suggesting that AG1478 has no effect on early/recycling endosomes as BFA. In addition, the treatment with AG1478 had no effect on the distribution of lysosomes systems, as marked by LAMP3, similar to that of BFA (Fig. 4L). Because of these similarities and differences, we conclude that AG1478 might target a similar target as BFA in dispersing the Golgi, but AG1478 might be more selective as it does not affect the endosomal compartment.

AG1478 blocks ARF1 activity in human cells—Our data described above suggest that in

AG1478 treated cells, ARF1 might reside in an inactive state in the cytosol, similar to that of BFA treated cells. To measure the ARF1 activity in AG1478-treated cells, we used an ARF1-GTP pull-down assay which monitors the amount of ARF1-GTP using a GST-GGA₃-GAT domain fusion protein (21,22). The GAT domain of GGA₃, an effector of ARF1, preferentially binds the active ARF1-GTP over the inactive ARF1-GDP. Treatment with AG1478 and BFA for 1 h dramatically reduced the amount of ARF1-GTP compared to that of control cells (Fig. 5A). On the other hand, although the treatment of BFA reduced the amount of active ARF1 in Rat2 cells as predicted, incubation of Rat2 cells with AG1478 had no effect on the levels of active ARF1 even if in the presence of high concentration of AG1478 (140 μ M). The species specificity of AG1478 on the human and rodent cells in reducing the amount of active ARF1 is consistent with its Golgi dispersing activity as described above and supports our hypothesis that AG1478 causes Golgi disassembly by blocking ARF1 activation in human cells.

Aluminum fluoride (AlFx) has been shown to activate the GDP-bound α subunit of heterotrimeric G-protein, and trigger the conversion to the GTP-bound state. By stabilizing a subset of ARF1 on the Golgi membrane, AlFx was shown to slow the dissociation of ARF1 from the Golgi membrane in the presence of BFA (40-42). Consistent with our hypothesis that AG1478 inhibits the activation of ARF1, we found that the treatment with AlFx significantly inhibited the Golgi dispersing effect of AG1478 (Fig. 5B).

The effects of AG1478 on GBF1—Since GBF1 has been shown to be stabilized on the VTCs and Golgi membrane in BFA treated cells, we performed subcellular fractionation experiment in H4 cells treated with AG1478 and BFA. In control cells, most of the endogenous GBF1 was

in the cytoplasmic fractions. As previously observed (23,33), the treatment of BFA caused a dramatic redistribution of GBF1 from cytoplasmic to membrane fraction (Fig. 6A). The treatment of AG1478 also led to a similar increase of GBF1 in the membrane fractions and a corresponding reduction in the cytoplasmic fractions, indicating that AG1478 may also lead to stabilization of GBF1 on membranes (Fig. 6A).

We further determined the effect of overexpressing GBF1 on the Golgi dispersing effect of AG1478. Overexpression of GBF1 has been shown to reduce the sensitivity of cells to BFA (43). GBF1-GFP was localized to both cytoplasm and the Golgi in H4 cells that were transiently transfected with an expression construct of GBF1-GFP (Fig. 6C) (33,44). Expression of GBF1 at low levels had no effect on the localization of COPI to the *cis*-Golgi. The treatment with AG1478 (14 μ M) for 30 min led to the rapid release of COPI into cytosol in control H4 cells but was ineffective in GBF1-GFP expressing H4 cells. Thus, overexpression of GBF1 prevents the release of COPI induced by AG1478, similarly to the effect seen with BFA. Consistent with a protective effect by GBF1, increased amounts of ARF1-GTP were found in cells overexpressing GBF1 compared to control cells in the presence of AG1478 (Fig. 6B). These observations indicate that overexpression of GBF1 also confers resistance to AG1478 induced Golgi disassembly.

Prolonged treatment of cells with 5 μ M BFA led to the redistribution of GBF1 into the ER (Fig. 6D) (33,43). Interestingly, the treatment with 14 μ M AG1478 for 1 h led to the appearance of GBF1-GFP in smaller punctate structures throughout the cell and larger bright clusters around the nucleus, which persisted even after longer treatment (4 h) at high concentration (42 μ M) (Fig. 6D). Thus, AG1478, in contrast to BFA,

is unable to localize GBF1-GFP into the reticular network. The small punctate structures labeled by GBF1-GFP in the presence of AG1478 resemble the structures formed by the catalytically inactive GBF1 mutant E794K (Fig. 6E) (44).

E794K mutation, which caused a change-reversal at the edge of a hydrophobic catalytic guanine nucleotide exchange center, has been shown to completely abolish the nucleotide exchange activity and stabilize the interaction between the mutant GEF and ARF1-GDP (45,46). The expression of E794K GBF1 causes the complete disassembly of the Golgi, similar to that of BFA-treated cells, while E794K GBF1 itself is known to be localized to the VTCs adjacent to the ERES (44). The treatment of BFA caused redistribution of E794K GBF1 from the VTCs adjacent to ERES into the ER (23,44). In striking contrast, the punctate dots of E794K GBF1-GFP were resistant to the effect of AG1478 (Fig. 6E), suggesting that different from that of BFA, AG1478 is unable to redistribute E794K GBF1 from the VTCs adjacent to the ERES into the ER. Taken together, we conclude that the treatment of AG1478 induces wt GBF1-GFP to phenocopy the E794K GBF1 mutant. Furthermore, the interaction of AG1478 with GBF1 most likely requires the catalytic activation of the Sec7 domain in GBF1. On the other hand, the catalytic activity of the Sec7 domain in GBF1 is not required for BFA to induce the redistribution of E794K mutant from the VTCs adjacent to the ERES into the ER.

The requirement of the Sec7 domains of GBF1 for the activity of AG1478—In addition to the Sec7 domain, GBF1 contains two non-catalytic domains (DCB and HUS) at its N-terminus, and three additional non-catalytic domains of its C-terminus (HDS1, HDS2 and HDS3) (Fig. 7A) (47,48). To gain more insight into the domains of GBF1 that are responsible for the effect of AG1478, we made two deletion constructs from

GBF1-GFP plasmid without the C-terminal domain. The GBF1-1-GFP construct contains the DCB, HUS and parts of the Sec7 domain while the GBF1-2-GFP comprises the DCB, HUS and the entire Sec7 domain. Both GBF1-1-GFP and GBF1-2-GFP were localized to the cytosol in a homogeneous manner and did not induce Golgi disassembly (data not shown). The treatment with BFA or AG1478 did not cause any significant change in GBF1-1-GFP distribution (Fig. 7B). Interestingly, the treatment with AG1478 induced GBF1-2-GFP to form peripheral punctate structures, similar to those seen with the E794K mutant (Fig. 6E). On the other hand, the addition of BFA redistributed GBF1-2 into a reticular network, most likely the ER, without any obvious punctate structure (Fig. 7C). Since GBF1-2-GFP but not GBF1-1-GFP contains an intact Sec7 domain, this result is consistent with the requirement of the Sec7 domain in interaction with AG1478. The requirement of an intact Sec7 domain suggests that AG1478 targets the Sec7 domain directly, or a binding protein of the Sec7 domain; alternatively, the deletion could indirectly affect the targeting of AG1478 by affecting the overall structure of GBF1. These possibilities need to be examined in future.

To characterize the peripheral punctate structures to which GBF1-2 localizes in the presence of AG1478, we used small molecules that are known to have effects on the Golgi. H89, a PKA inhibitor, was shown to block COPII recruitment to ER membrane. The “Golgi remnants” localized to VTCs adjacent to ERES induced by BFA could be redistributed to ER after combined treatment with BFA and H89 (49,50). Treatment with H89 and AG1478 together in H4 cells redistributed the peripheral punctate structures of GBF1-2-GFP to the ER, suggesting that GBF1-2 punctates formed upon AG1478 treatment may also be localized to VTCs adjacent

to ERES (Fig. 7D).

Since the treatment of BFA led to the redistribution of GBF1-2-GFP into a reticular network, we tested if BFA can further redistribute the punctate structures formed by GBF1-2-GFP upon AG1478 treatment. As shown in Fig. 7D, the addition of BFA after AG1478 treatment led to the redistribution of the punctate structures of GBF1-2-GFP into a reticular network, likely corresponding to the ER. On the other hand, the addition of AG1478 after the treatment of BFA was not able to induce GBF1-2-GFP to form punctate structures. Thus, the effect of BFA is dominant over that of AG1478.

The VTCs adjacent to the ERES can be differentiated by the presence of ERGIC53 and COP II marker (44,51). To further characterize the peripheral punctate structures of GBF1-2-GFP and GBF1-GFP induced by AG1478, we examined their distribution relative to that of ERGIC53 and Sec13, which are markers for the VTCs and the ERES, respectively. The punctate spots of GBF1-2-GFP and GBF1-GFP induced by AG1478 overlapped almost completely with ERGIC53 (Fig. 8A and 8C) but only partially with that of Sec13 (Fig. 8B and 8D). Together, these results confirm that AG1478 treatment causes the accumulation of GBF1 and GBF1-2 on the VTCs adjacent to the ERES, whereas the treatment of BFA is known to cause the complete redistribution of GBF1 into the ER network.

DISCUSSION

We screened a small molecule library to identify new molecules that affect the Golgi for reagents as tools to study intracellular membrane trafficking. We identified a novel activity of known compound, AG1478, in down-regulation of the ARF1 activity, which in turn leads to the dispersal of the Golgi structure. The effect of

AG1478 on the *cis*-Golgi is more selective than that of BFA and AG1478 does not affect the endosomal systems as BFA does. We show that the Golgi dispersing effect of AG1478 can be partially suppressed by the overexpression of GBF1, a large GEF that promotes the GDP to GTP exchange of ARF1. This effect is similar to that of BFA. Interestingly, however, in contrast to BFA, AG1478 was unable to disperse overexpressed GBF1 from the peripheral VTCs adjacent to the ERES into the ER. Instead, in the presence of AG1478, wt GBF1-GFP forms punctate structures on the VTCs adjacent to the ERES, a phenotype similar to that with the E794K GBF1-GFP mutant. We conclude that AG1478 is likely to target a molecular entity that regulates the Sec7 nucleotide exchange activity of GBF1 in human cells but not rodent, canine or kangaroo rat cells.

The ARF family of GTPases plays a central role in maintaining Golgi structure and function. Six ARF isoforms (ARF1-6) in mammals can be classified into three classes based on their primary sequences; however, ARF2 is lost in the human genome. ARF isoforms exhibit similar biochemical activities in regulating membrane traffic (52,53). ARF1, the best-characterized ARF, localizes primarily to the Golgi complex and regulates several types of coat proteins. Our results demonstrate that Golgi disassembly induced by AG1478 is caused by inhibition of ARF1 activation. We show that ARF1 exists in an inactive state localized in the cytosol of AG1478 treated cells, indicating a failure in the recruitment of ARF1 to membranes to facilitate COPI transport. The amount of active ARF1-GTP production in H4 human cells was dramatic decreased after AG1478 treatment.

The selective effect of AG1478 on the *cis*-Golgi associated proteins led us to first examine the role of GBF1, which is the only GEF localized at the *cis*-Golgi. GBF1 is a high

molecular weight GEF that cycle rapidly on and off the Golgi membrane. The mobility of GBF1 is associated with its exchange activity as an inactive mutant E794K cycles slower and stabilizes on membrane longer than wtGBF1 (23). Szul et al. propose that GBF1 is stabilized on membrane when in a complex with ARF1-GDP and the catalytic activity of GBF1 is required for its dissociation from ARF and membrane (23). Since the treatment of AG1478 led to an increased association of GBF1 with the membrane, we propose that AG1478 also inhibits the catalytic activity of GBF1 and in the presence of AG1478, GBF1 is also stabilized on the membrane in complex with ARF1-GDP.

GBF1 is localized to the peripheral VTCs and the juxta-nuclear early Golgi in normal mammalian cells (33,44). However, the anti-GBF1 antibody that we used does not recognize the endogenous GBF1 in peripheral puncta on the VTCs in control cells (Fig. 4C) as demonstrated elegantly by the affinity purified anti-GBF1 antibody by Paul and Sztul (33,44). AG1478 can not disperse the transfected wtGBF1 from the VTCs (Fig. 6D), which mimics the behavior of the E794K GBF1 mutant. On the other hand, the treatment of BFA can disperse E794K from the VTCs into the ER (44). Thus, the treatment of AG1478, but not that of BFA, provides a phenocopy of the Sec7 mutant GBF1. A time-lapsed imaging analysis showed that the dispersal of GBF1-GFP induced by BFA occurs in two steps: a transient accumulation of GBF1-GFP in both peripheral puncta and juxta-nuclear Golgi area, and a subsequent dispersal into the ER (33). Thus, the treatment of AG1478 might arrest the GBF1-GFP at the first step. Since GBF1 knockdown also blocks cargo in peripheral VTCs structures (51), it has been proposed that inactive GBF1 is localized to the VTCs adjacent to the ERES. We propose that AG1478 selectively

targets the Sec7 activity of GBF1 and traps GBF1 on VTCs adjacent to the ERES, whereas BFA inhibits not only the nucleotide exchange activity of GBF1 but also an additional step that is independent of Sec7 activity and leads to the dispersal of GBF1 into the ER. For example, BFA might work with multiple GEFs, each affecting a different compartment including the compartment to which E794K targets, thereby changing its distribution. On the other hand, the effect of AG1478 might be more selective. Therefore, AG1478 might provide a useful tool in defining an intermediate vesicular trafficking step that can be only transiently observed using BFA. The low cytotoxicity of AG1478 also suggests that the cytotoxicity of BFA might not be directly related to its inhibitory effect on the Sec7 nucleotide exchange activity. Since BFA has been proposed to inhibit additional targets to affect the endosomal system (14-16) while AG1478 does not have such side effects, it is possible that the inhibitory effect of BFA on its additional target(s) involved in the endosomal trafficking leads to its cytotoxicity.

The selectivity of AG1478 for human cells is also interesting. One might speculate that such selectivity is caused by species difference in the target of AG1478. Alternatively, the presence of ARF2 isoform in rodent cells but not human cells might explain the resistance of rodent cells to AG1478. To test the latter possibility, we have used small interfering RNA (siRNA) to decrease expression of ARF2 in Rat2 cells. However, the expression of siRNA for ARF2 did not sensitize the rodent cells to AG1478 (data not shown). We have also considered the possibility that GBF1 is the direct target of AG1478. Since the Sec7 domains of human and mouse GBF1 proteins are highly similar with 96% identity at the amino acid level, we made an expression construct expressing a h(m)GBF1-2 fusion protein which contains the Sec7 domain of mouse GBF1 with other domains

of human GBF1. AG1478 treatment redistributed this h(m)GBF1-2 to the VTCs adjacent to the ERES in H4 cells, similar to the effect seen with the wild type (data not shown), suggesting that differences in the Sec7 domains of GBF1 between mouse and human cannot account for the resistance in rodent cells.

In conclusion, we have identified a novel Golgi dispersing molecule AG1478. We show that similar to BFA, AG1478 inhibits the activity of ARF1. AG1478 exhibits a number of interesting properties distinct from that of BFA. First, AG1478 exhibits low cytotoxicity whereas BFA is highly toxic. Second, the Golgi dispersing effect of AG1478 is highly species specific, whereas BFA

can affect both human and rodent cells. Third, AG1478 preferentially targets the *cis*-Golgi compartment whereas BFA targets both the *cis*- and *trans*-Golgi. Fourth, AG1478 redistributes GBF1 to the peripheral VTCs adjacent to that of ERES but not into the ER, mimicking the phenotype of the E794K GBF1 mutant; whereas BFA can disperse the E794K mutant into the ER network. Since the interaction of AG1478 with GBF1 depends upon a functional Sec7 domain, we propose that AG1478 provides an interesting new tool to define the functional role of nucleotide exchange factors.

REFERENCES

1. Rothman, J. E. (1994) *Nature* **372**, 55-63
2. Schekman, R. a. O., L. . (1996) *Science* **271**, 1526-1533
3. Hauri, H. P., Kappeler, F., Andersson, H., and Appenzeller, C. (2000) *J. Cell Sci.* **113**, 587-596
4. Ward, T. H., Polishchuk, R.S., Caplan, S., Hirschberg, K., and Lippincott-Schwartz, J. (2001) *J Cell Biol.* **155**, 557-570
5. Altan-Bonnet, N., Sougrat, R. and Lippincott-Schwartz, J. (2004) *Curr. Opin. Cell Biol.* **16**, 364-372
6. D'Souza-Schorey, C., and Chavrier, P. (2006) *Nat. Rev. Mol. Cell Biol.* **7**, 347-358
7. Donaldson, J. G., Honda, A., and Weigert, R. (2005) *Biochim Biophys Acta.* **1744**, 364-373
8. Claude, A., Zhao, B.P., Kuziemsky, C.E., Dahan, S., Berger, S.J., Yan, J.P., Arnold, A.D., Sullivan, E.M., and Melançon, P. (1999) *J. Cell Biol.* **146**, 71-84
9. Kawamoto, K., Yoshida, Y., Tamaki, H., Torii, S., Shinotsuka, C., Yamashina, S., and Nakayama, K. (2002) *Traffic.* **3**, 483-495
10. Renault, L., Guibert, B., and Cherfils, J. (2003) *Nature* **426**, 525-530
11. Mossessova, E., Corpina, R.A., and Goldberg, J. (2003) *Mol. cell* **12**, 1403-1411
12. Tsai, S. C., Adamik, R., Haun, R.S., Moss, J., and Vaughan, M. (1993) *J. Biol. Chem.* **268**, 10820-10825
13. Dinter, A., and Berger, E.G. (1998) *Histochem. Cell Biol.* **109**, 571-590
14. Lippincott-Schwartz, J., Yuan, L., Tipper, C., Amherdt, M., Orci, L., and Klausner, R.D. (1991) *Cell* **67**, 601-616
15. Wood, S. A., Park, J. E., and Brown, W. J. (1991) *Cell* **67**, 591-600
16. Hunziker, W., Whitney, J.A., and Mellman, I. (1991) *Cell* **67**, 617-627
17. Guo, H., Tittle, T.V., Allen, H., and Maziarz, R.T. (1998) *Exp. Cell Res.* **245**, 57-68

18. Citterio, C., Vichi, A., Pacheco-Rodriguez, G., Aponte, A.M., Moss, J., and Vaughan, M. (2008) *Proc. Natl. Acad. Sci. (U S A)* **105**, 2877-2882
19. Brewer, C. B., and Roth, M.G. (1995) *J. Cell Sci.* **108**, 789-796
20. Smith, K., Gunaratnam, L., Morley, M., Franovic, A., Mekhail, K., and Lee, S. (2005) *Cancer Res.* **65**, 5221-5230
21. Shinotsuka, C., Yoshida, Y., Kawamoto, K., Takatsu, H., and Nakayama, K. (2002) *J. Biol. Chem.* **277**, 9468-9473
22. Yoon, H. Y., Bonifacino, J.S., and Randazzo, P.A. (2005) *Methods Enzymol.* **404**, 316-332
23. Szul, T., Garcia-Mata, R., Brandon, E., Shestopal, S., Alvarez, C., and Sztul, E. (2005) *Traffic.* **6**, 374-385
24. Nakamura, N., Rabouille, C., Watson, R., Nilsson, T., Hui, N., Slusarewicz, P., Kreis, T.E., and Warren, G. (1995) *J Cell Biol.* **131**, 1715-1726
25. Carpenter, A. E., Jones, T.R., Lamprecht, M.R., Clarke, C., Kang, I.H., Friman, O., Guertin, D.A., Chang, J.H., Lindquist, R.A., Moffat, J., Golland, P., and Sabatini, D.M. . (2006) *Genome Biology* **7**, R100
26. Lamprecht MR, S. D., and Carpenter AE (2007) *Biotechniques* **42**, 71-75
27. Daub, H., Weiss, F.U., Wallasch, C., and Ullrich, A. (1996) *Nature* **379**, 557-560
28. Levitzki, A., and Gazit, A. (1995) *Science* **267**, 1782-1788
29. Low, S. H., Wong, S.H., Tang, B.L., Tan, P., Subramaniam, V.N., and Hong, W. (1991) *J Biol Chem.* **266**, 17729-17732
30. Ktistakis, N. T., Roth, M.G., and Bloom, G.S. (1991) *J Cell Biol.* **113**, 1009-1023
31. Donaldson, J. G., Kahn, R.A., and Lippincott-Schwartz, J., Klausner, R.D. (1991) *Science* **254**, 1197-1199
32. Rabouille, C., and Klumperman, J. (2005) *Nat. Rev. Mol. Cell Biol.* **6**, 812-817
33. Zhao, X., Claude, A., Chun, J., Shields, D.J., Presley, J.F., and Melançon, P. (2006) *J. Cell Sci.* **119**, 3743-3753
34. Hammond, A. T., and Glick, B.S. (2000) *Mol. Biol. Cell.* **11**, 3013-3030
35. Tang, B. L., Peter, F., Krijnse-Locker, J., Low, S.H., Griffiths, G., and Hong, W. (1997) *Mol. Cell Biol.* **17**, 256-266
36. Orci, L., Perrelet, A., Ravazzola, M., Wieland, F.T., Schekman, R., and Rothman, J.E. (1993) *Proc. Natl. Acad. Sci. (U S A).* **90**, 11089-11093
37. Seemann, J., Jokitalo, E., Pypaert, M., and Warren, G. (2000) *Nature* **407**, 1022-1026
38. Gleeson, P. A., Anderson, T.J., Stow, J.L., Griffiths, G., Toh, B.H., and Matheson, F. (1996) *J. Cell Sci* **109**, 2811-2821
39. Stephen, G. M., Lucinda, C., and Hsiao-Ping, H. M. (1992) *J. Cell Biol.* **118**, 267-283
40. Rittinger, K., Walker, P.A., Eccleston, J.F., Smerdon, S.J., and Gamblin, S.J. (1997) *Nature* **389**, 758-762
41. Finazzi, D., Cassel, D., Donaldson, J.G., and Klausner, R.D. (1994) *J Biol Chem.* **269**, 13325-13330
42. Feng, Y., Yu, S., Lasell, T.K., Jadhav, A.P., Macia, E., Chardin, P., Melancon, P., Roth, M., Mitchison, T., and Kirchhausen, T. (2003) *Proc. Natl. Acad. Sci. (U S A)* **100**, 6479-6474

43. Niu, T. K., Pfeifer, A.C., Lippincott-Schwartz, J., and Jackson, C.L. (2005) *Mol. Biol. Cell.* **16**, 1213-1222
44. García-Mata, R., Szul, T., Alvarez, C., and Sztul, E. (2003) *Mol. Biol. Cell* **14**, 2250-2261
45. Cherfils, J., Ménétrey, J., Mathieu, M., Le Bras, G., Robineau, S., Béraud-Dufour, S., Antony, B., and Chardin, P. (1998) *Nature* **392**, 101-105
46. Mossessova, E., Gulbis, J.M., and Goldberg, J. (1998) *Cell* **92**, 415-423
47. Mouratou, B., Biou, V., Joubert, A., Cohen J, Shields DJ, Geldner N, Jürgens G, Melançon P, and Cherfils J. (2005) *BMC Genomics.* **17**
48. Ramaen, O., Joubert, A., Simister, P., Belgareh-Touzé, N., Olivares-Sanchez, M.C., Zeeh, J.C., Chantalat, S., Golinelli-Cohen, M.P., Jackson, C.L., Biou, V., and Cherfils, J. (2007) *J. Biol. Chem.* **282**, 28834-28842
49. Lee, T. H., and Linstedt, A.D. (2000) *Mol. Biol. Cell.* **11**, 2577-2590
50. Puri, S., and Linstedt, A.D. (2003) *Mol. Biol. Cell.* **14**, 5011-5018
51. Manolea, F., Claude, A., Chun, J., Rosas, J., and Melançon, P. (2008) *Mol. Biol. Cell.* **19**, 523-535
52. Chun, J., Shapovalova, Z., Dejgaard, S.Y., Presley, J.F., and Melançon, P. (2008) *Mol. Biol. Cell.* **Jun 4**
53. Volpicelli-Daley, L. A., Li, Y., Zhang, C.J., and Kahn, R.A. (2005) *Mol. Biol. Cell.* **16**, 4495-4508

FOOTNOTES

*We are grateful to Dr. Tom Rapoport (Harvard Medical School) and Drs. Lippincott-Schwartz (National Institutes of Health, Bethesda) for critical reading and editing of this manuscript. We thank Renxiao Wang (Shanghai Institute of Organic Chemistry) for model analysis and helpful discussion. We express our deep appreciation for the kind gifts of plasmids and antibodies from Drs. Lippincott-Schwartz (National Institutes of Health, Bethesda), Elizabeth Sztul (University of Alabama, Birmingham), Benjamin S. Glick (University of Chicago, Chicago), Hans-Peter Hauri (University of Basel, Basel), Paul A. Randazzo (National Institutes of Health, Bethesda) and Wanjin Hong (Institute Molecular Biology, Singapore). This work was supported in part by grants from the National Natural Science Foundation of China (20321202), the Chinese Academy of science (KGCX2-SW-209) to D. M. and from the National Institute on Aging (U.S.) to J. Y. (R37 AG12859). A.E.C was a Novartis fellow of the Life Sciences Research Foundation.

Abbreviations used:

AIF, Aluminum fluoride; ARF, ADP-ribosylation factor; BFA, Brefeldin A; COP, coatomer protein; DMSO, Dimethylsulfoxide; EGFR, Epidermal growth factor receptor; ERES, ER exit sites; ERGIC, ER-Golgi intermediate compartment; GBF1, Golgi-specific brefeldin A resistance factor 1; GEF, Guanine nucleotide exchange factor; GFP, Green fluorescent protein; VTCs, vesicular tubular clusters structure;

FIGURE LEGENDS

Fig. 1. AG1478 treatment causes Golgi fragmentation in H4 cells. H4-p58 cells (A) or H4 cells (C) were treated with DMSO or 14 μ M AG1478 as indicated for 1 h. H4 cells were fixed and stained with anti-GM130 antibody. (B) Chemical structures of AG1478 and BFA. (D-F) H4 cells were treated with DMSO or AG1478 for different concentrations, different time, then stained with an antibody against GM130. Images were analysed by CellProfiler software. Bar, 10 μ m.

Fig. 2. The effect of AG1478 on Golgi is independent of EGFR. (A) H4 cells were pretreated with AG1478 for 30 min, then treated with 50 ng/ml EGF for 5 min and analyzed for anti-phosphoEGFR (tyr1068) or tubulin by immunoblot. (B) Control western blot for the effect of EGFR siRNA. Anti-tubulin was used as a loading control. (C-F) H4 cells were co-transfected pEGFP-N1 plasmid with EGFR siRNA at 1:10 ratio for 24 h, then treated with DMSO or 14 μ M AG1478 as indicated for 1 h. H4 cells expressing EGFP siRNA (D and F) were stained with anti-GM130 antibody (C and E). GFP-positive transfected cells were indicated by white *. Bar, 10 μ m.

Fig. 3. Rat2 cells are resistant to AG1478 but not BFA. (A) Rat2 cells were treated with DMSO, 140 μ M AG1478 or 5 μ M BFA as indicated for 4h, stained with anti-GM130 antibody. (B) H4 cells or Rat2 cells were pretreated with 14 μ M AG1478 for 30 min or not, then stimulated by 50 ng/ml EGF for 5 min, and analyzed by western blotting using anti-phospho-EGFR (tyr1068), anti-phospho-ERK and anti-tubulin antibody. Bar, 10 μ m.

Fig. 4. Effects of AG1478 on the distribution of intracellular Golgi associated proteins. H4 cells expressing ARF1-GFP (A), Sec13-GFP (D), p58-YFP (E), GalT-CFP (G) were incubated with DMSO, 14 μ M AG1478, 5 μ M BFA for 1 h, or H4 cells incubated with DMSO, 14 μ M AG1478, 5 μ M BFA for 1 h, then stained with antibodies against β -COP (B), GBF1 (C), GM130 (F), p230 (H), Adaptin γ (I), Adaptin δ (J) and LAMP3 (L). (K) H4 cells incubated with Alexa 568-labeled transferrin for 5 min, then treated with DMSO, 14 μ M AG1478, 5 μ M BFA for 1h. Bar, 10 μ m.

Fig. 5. ARF1 inactivity causes Golgi disassembly induced by AG1478 on H4 cells. (A) ARF1-GTP pull down assay. H4 cells or Rat2 cells were transfected transiently with ARF1-GFP for 24 h, treated with DMSO (lane 1 and 5), 14 μ M AG1478 (lane 2 and 6), 140 μ M AG1478 (lane 3 and 7) and 5 μ M BFA (lane 4 and 8) for 1 h before lysis. The upper panel shows the amount of GTP bound ARF1-GTP, the lower panel shows the total amount of ARF1-GTP in cells. (B) H4 cells were pretreated with control or 50 μ M $AlCl_3$ and 30 mM NaF for 10 min as indicated, then treated with 14 μ M AG1478 or 1 μ M BFA as indicated together for 30 min. Cells were stained with an antibody against β -COP. Bar, 10 μ m.

Fig. 6. The effect of AG1478 on GBF1. (A) H4 cells were treated with DMSO (lane 1,4), 14 μ M AG1478 (lane 2,5), 5 μ M BFA (lane 3,6) for 1h, homogenized and subjected to differential centrifugation, equivalent amount of the cytosolic and membrane fractions were resolved by SDS-PAGE and Western blotted with anti-GBF1, anti-calnexin and anti-tubulin. (B) H4 cells were transfected with ARF1-GFP together with GBF1-GFP or pEGFP-C1 for 24h, then treated with DMSO, 14 μ M AG1478 for 30min. The cell lysates were analyzed by ARF1 pull down assay. (C) H4 cells were transfected transiently with

GBF1-GFP plasmid for 24 h, treated with DMSO, 14 μ M AG1478 or 1 μ M BFA for 30 min. Cells expressing GBF1-GFP were indicated by white *. Cells were stained with an antibody against β -COP. (D) H4 cells were transfected transiently with GBF1-GFP plasmid for 24 h, treated with DMSO, 14 μ M AG1478 or 5 μ M BFA for 1 h. (E) H4 cells were transfected transiently with E794K-GFP plasmid for 24 h, treated with DMSO, 14 μ M AG1478 or 5 μ M BFA for 1h. Bar, 10 μ m.

Fig. 7. The effect of AG1478 on the GBF1-1 protein. (A) Schematic representation of different deletion constructs from GBF1-GFP. (B-C) H4 cells were transfected with GBF1-1-GFP or GBF1-2-GFP for 24 h, then treated with DMSO, 14 μ M AG1478 or 5 μ M BFA as indicated for 1 h. (D) H4 cells were transfected with GBF1-2-GFP for 24 h, treated with DMSO, or pretreated with 14 μ M AG1478 for 1 h, then treated with 100 μ M H89 together with AG1478 for 10 min, or treated with 5 μ M BFA together with AG1478 for 1 h, or pretreated with 5 μ M BFA for 1 h, then treated with 14 μ M AG1478 together with BFA for 1 h. Bar, 10 μ m.

Fig. 8. AG1478 causes accumulation of GBF1-2 and GBF1 spots on VTCs. H4 cells were transfected with GBF1-2-GFP (A,B), GBF1-GFP (C,D) (green) alone or with ERGIC53-myc for 24 h, then treated with 14 μ M AG1478 for 1 h. Fixed cells were stained with an antibody against myc or sec13 (red). Single-slice confocal images are shown. Insets show a higher magnification of the boxed areas of merged images. Bar, 10 μ m.

Figure 1.

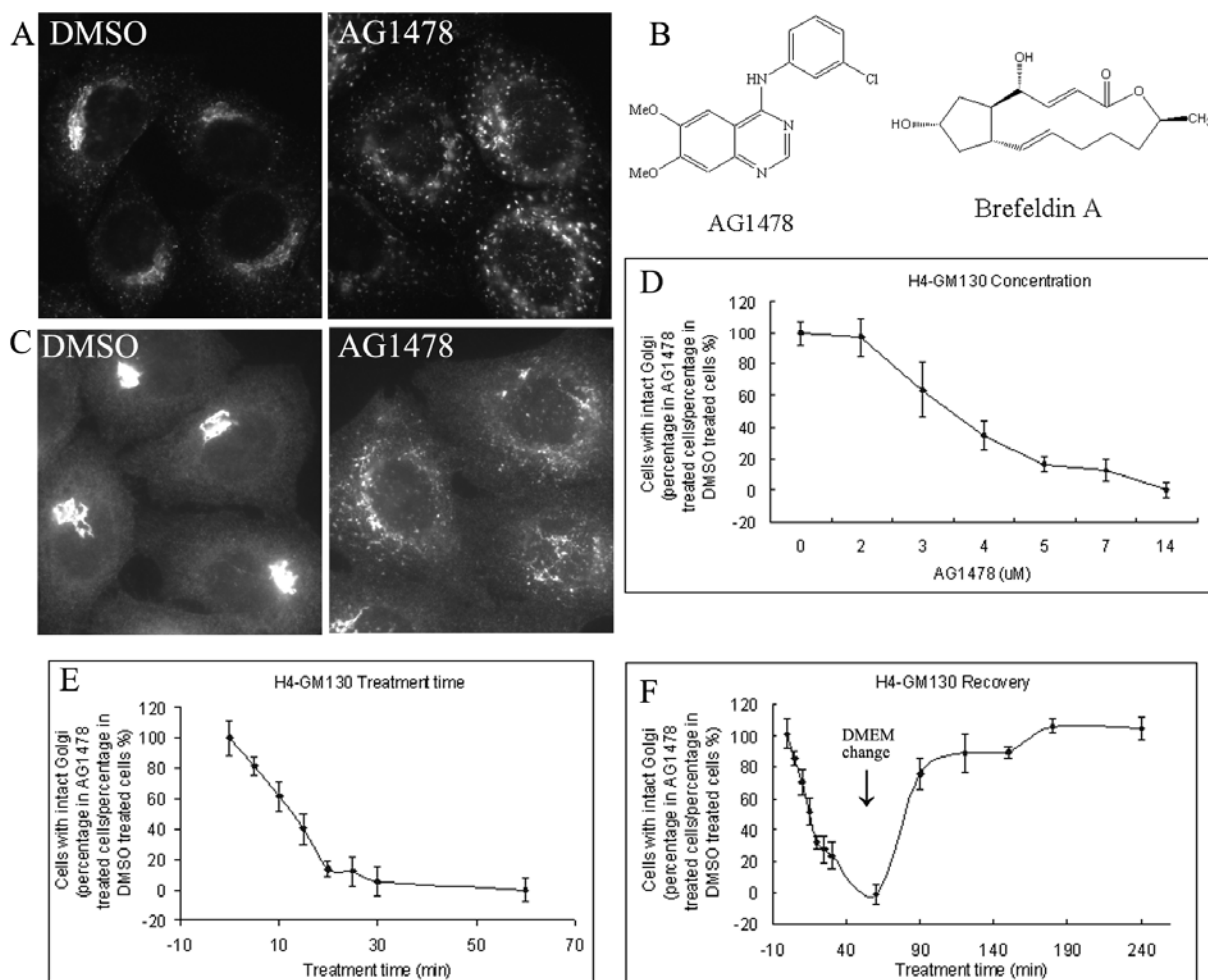


Figure 2.

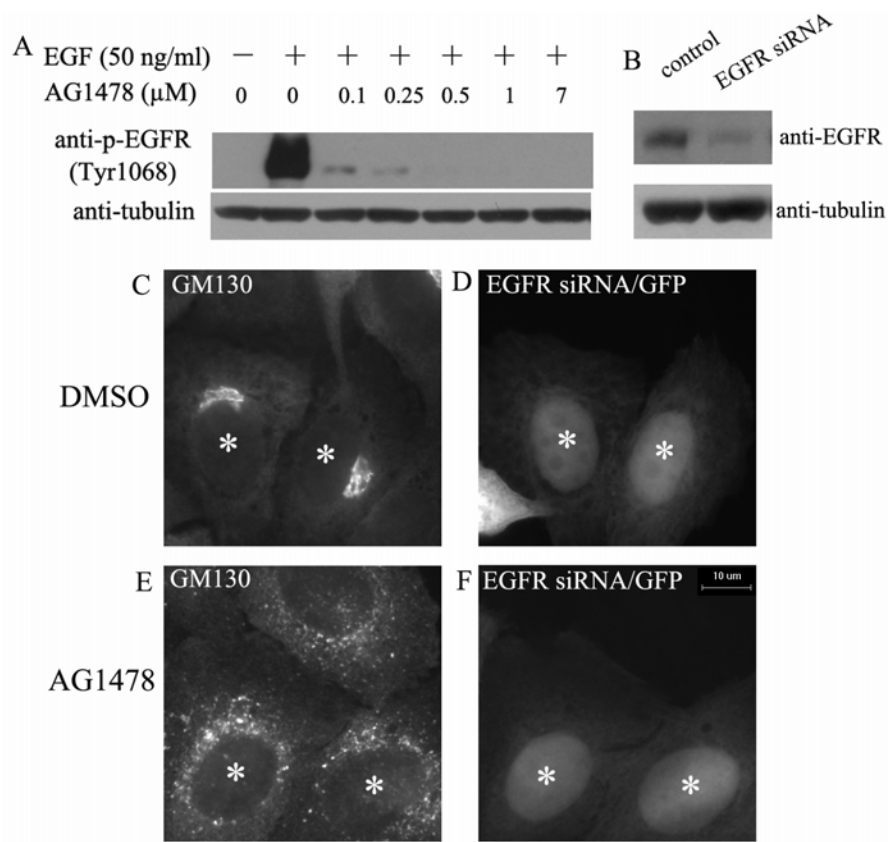


Figure 3.

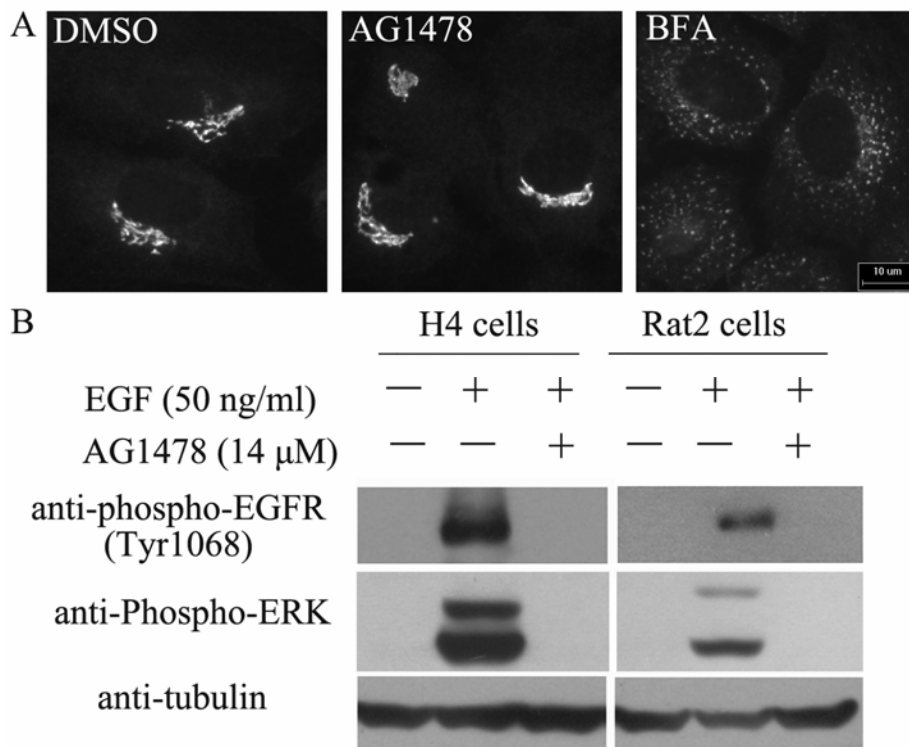


Figure 4.

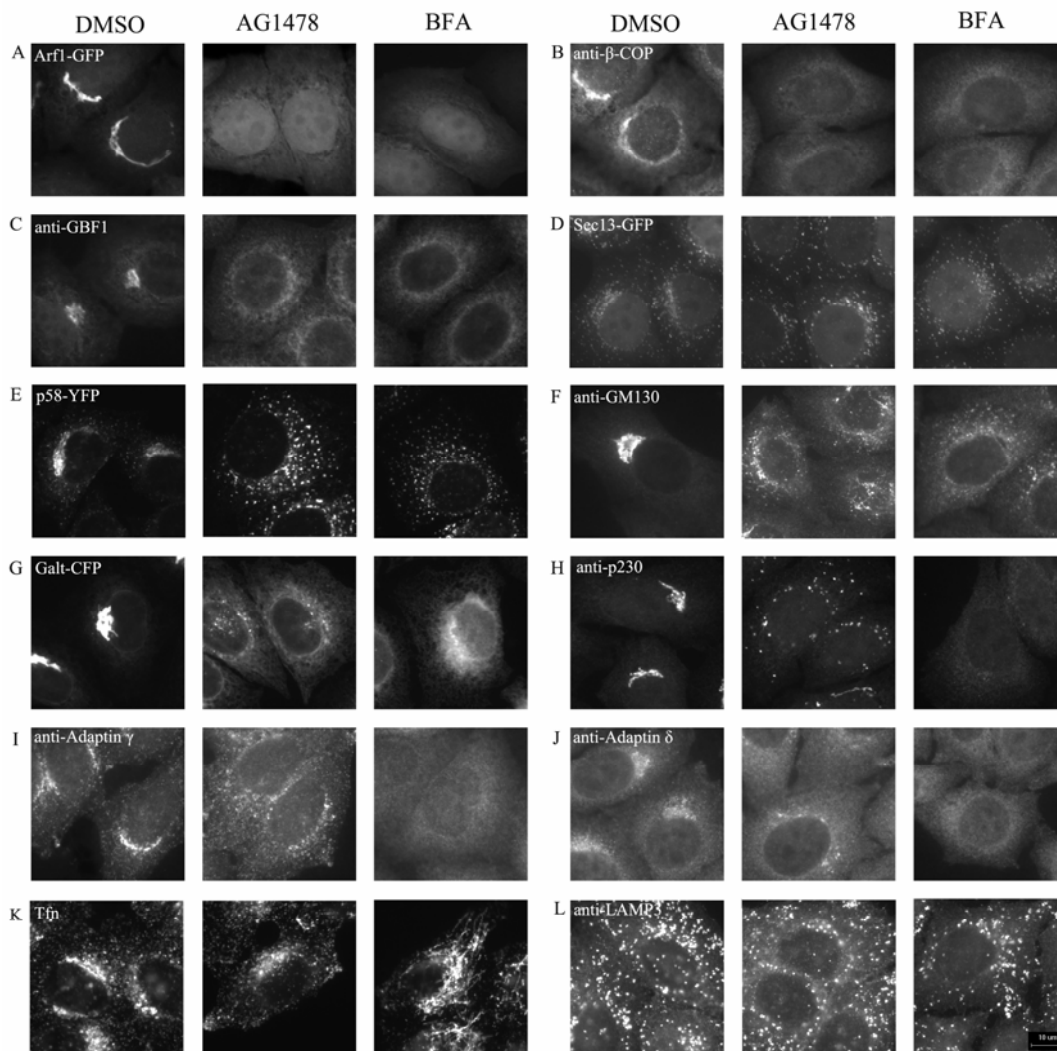


Figure 5.

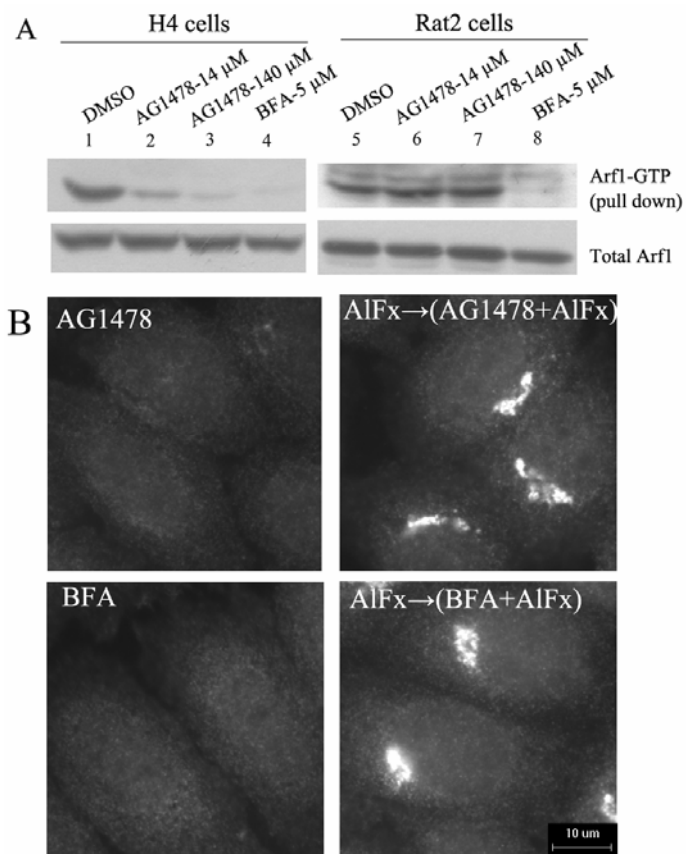


Figure 6.

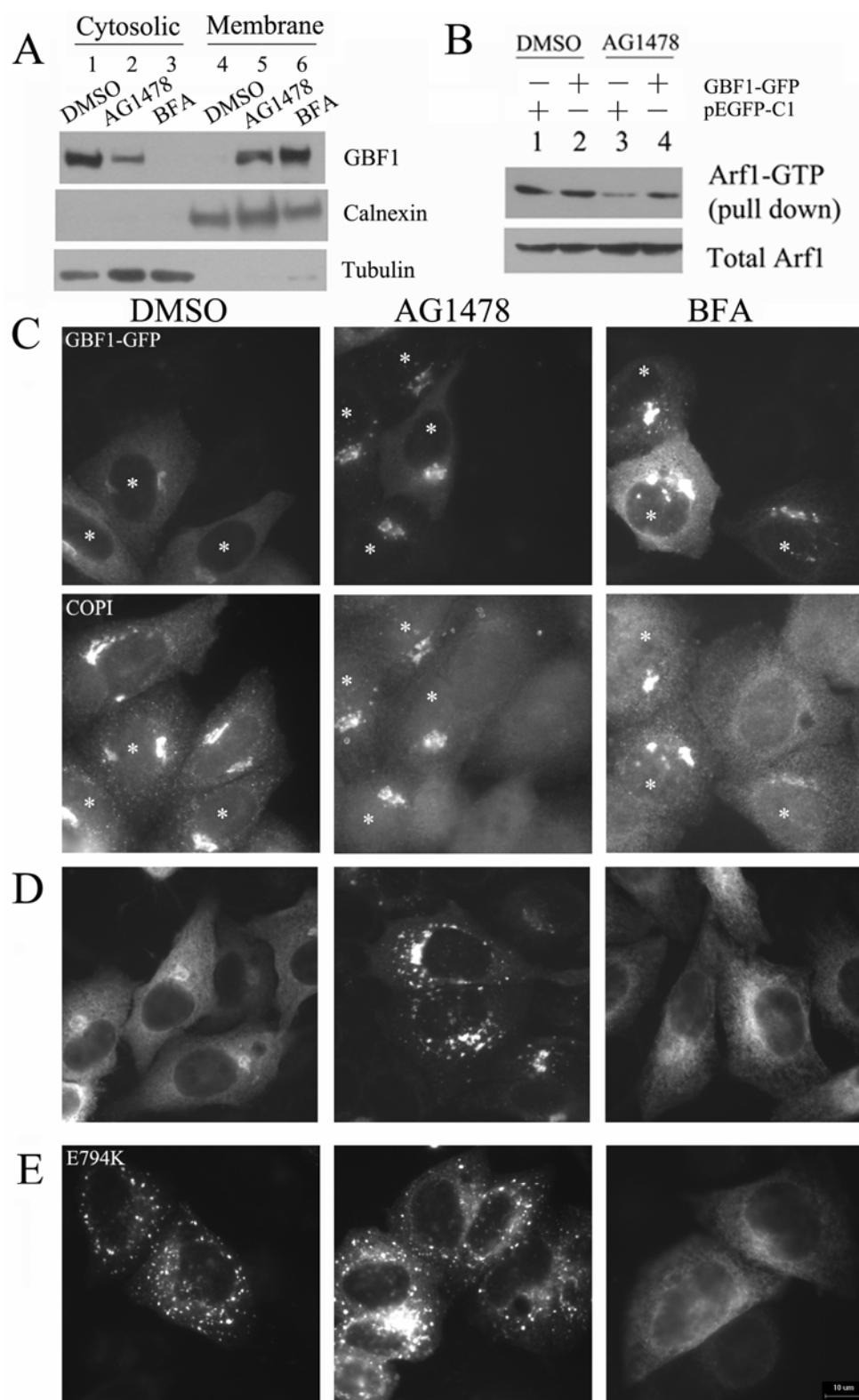


Figure 7

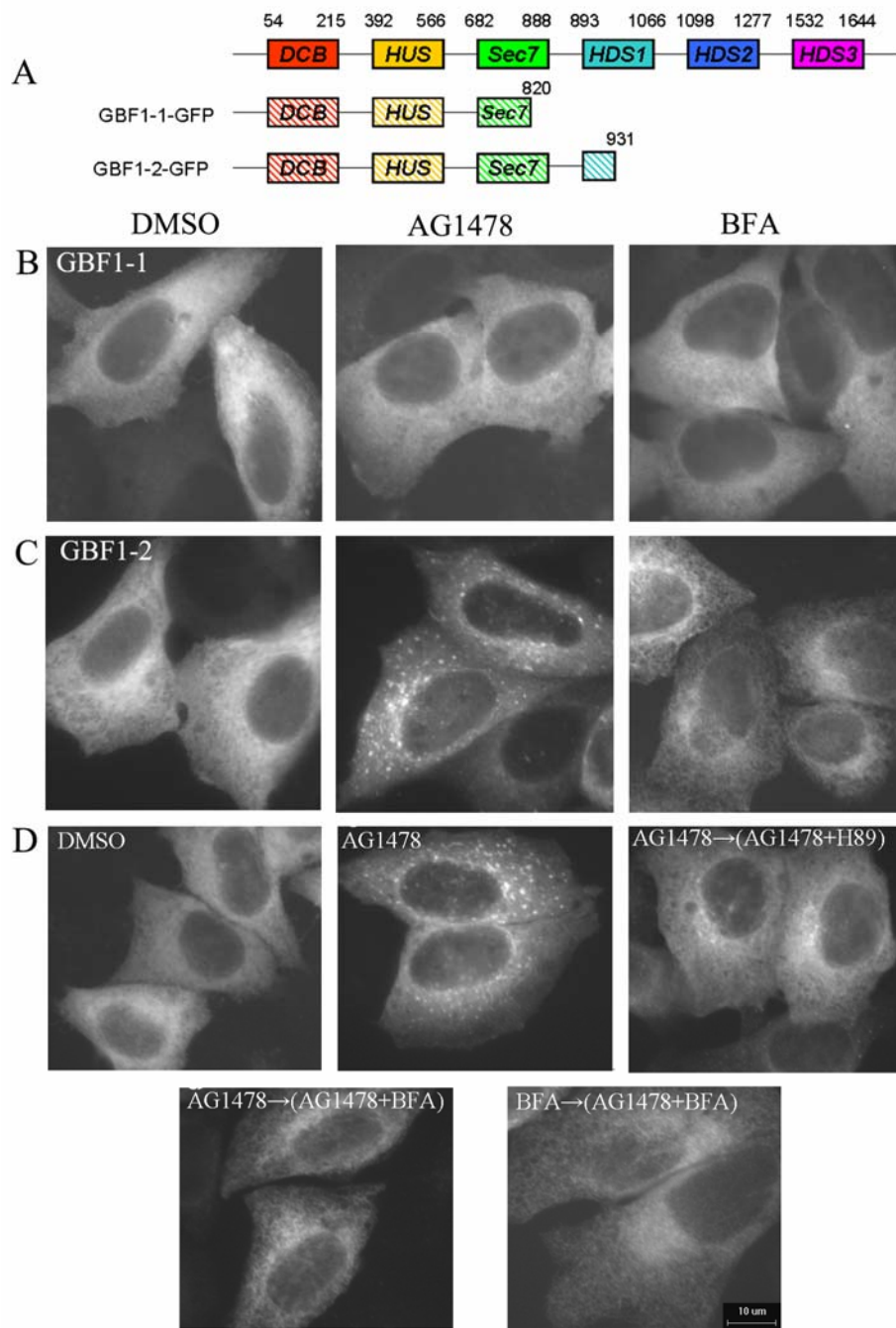
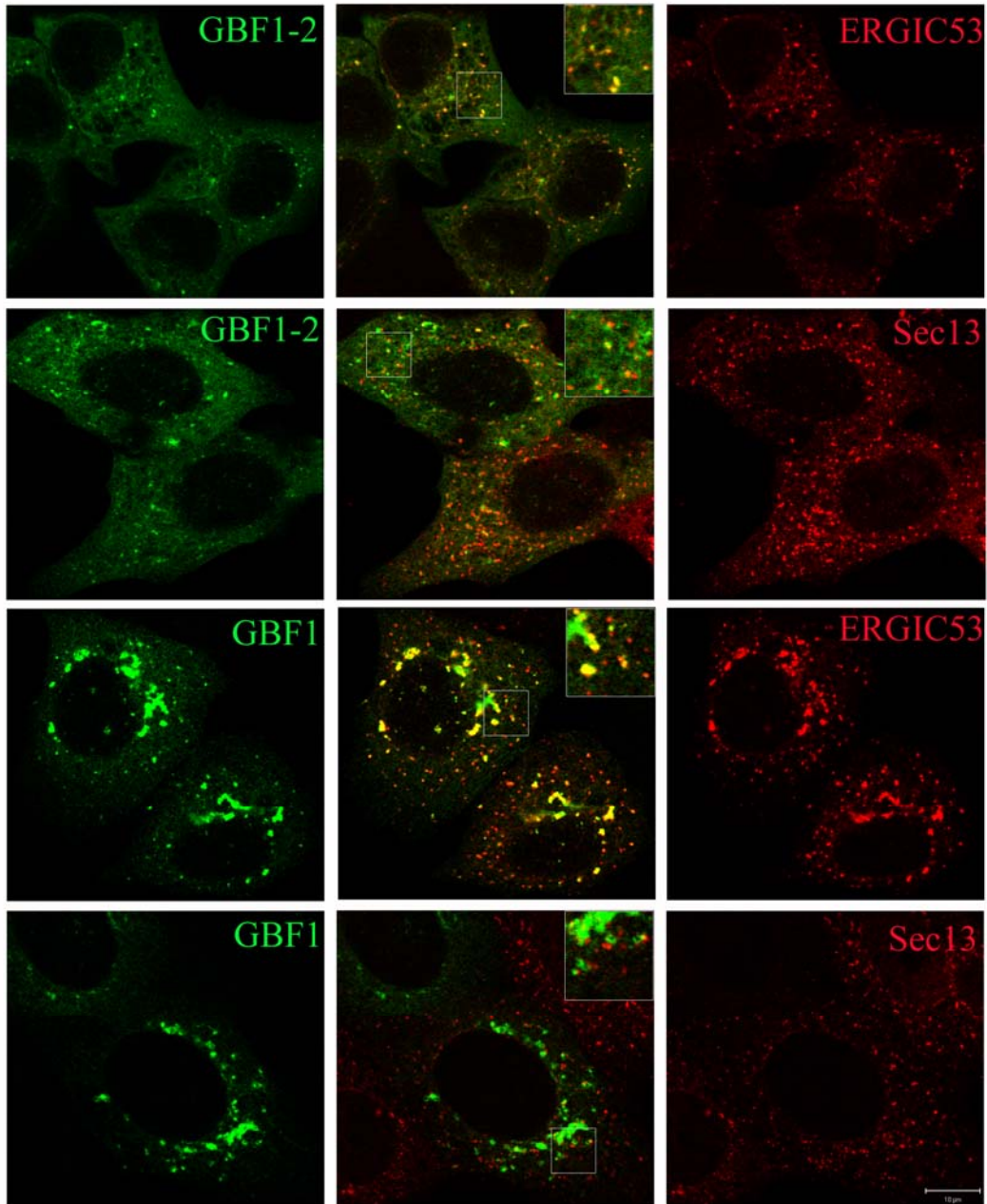
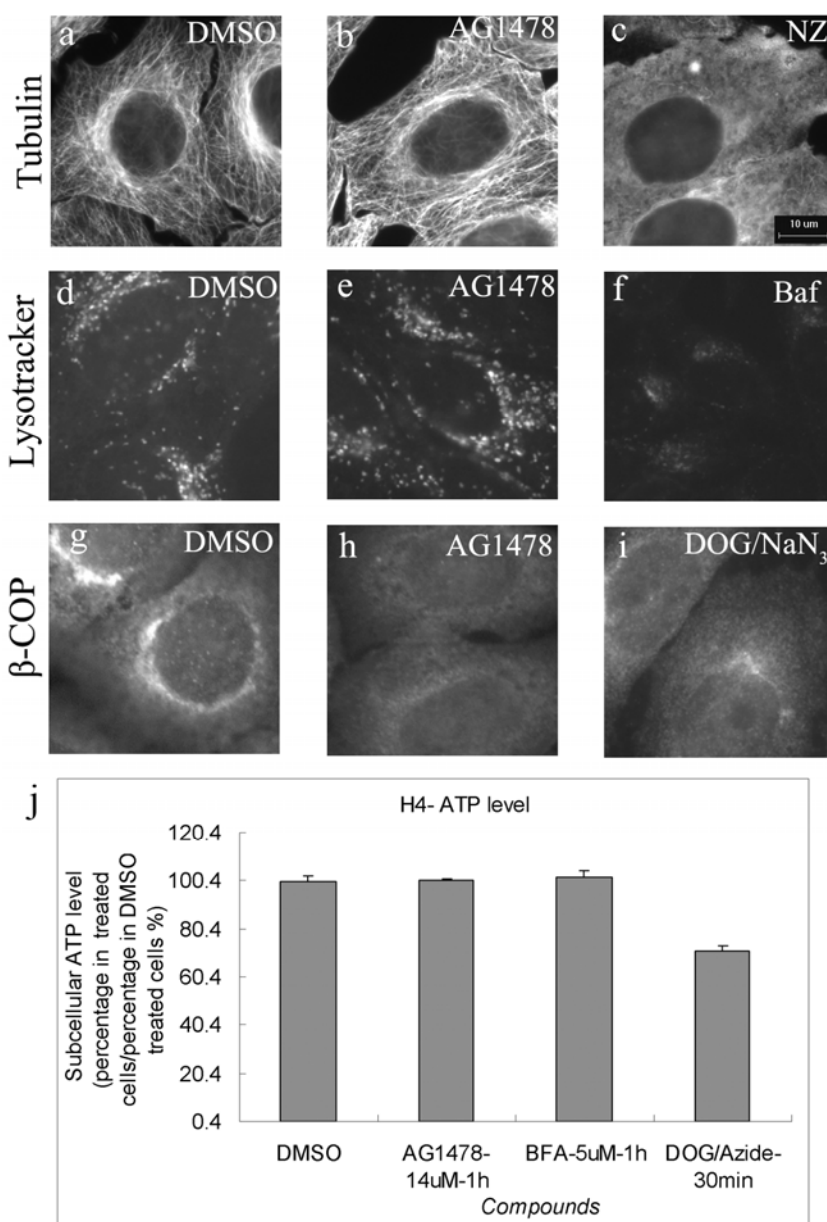


Figure 8

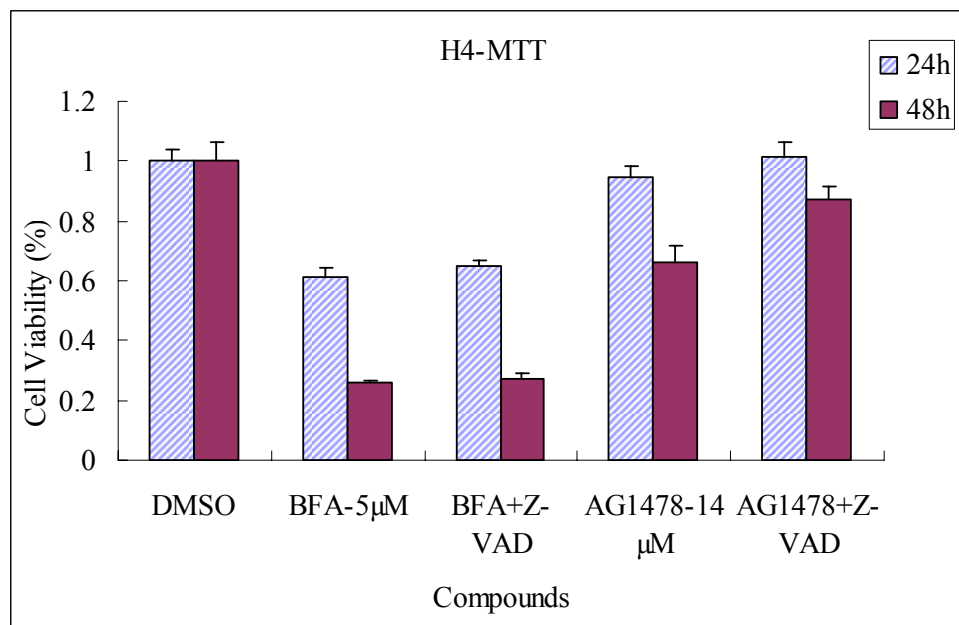


Supplemental Material:

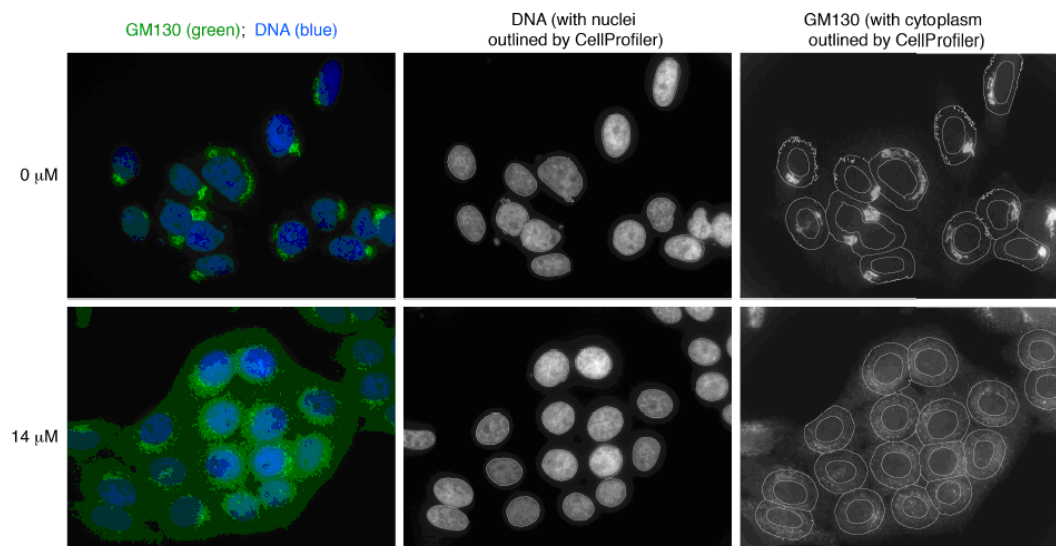
Supplemental Fig. 1 The effect of AG1478 on Tubulin, cellular pH and ATP level. H4 cells were treated with DMSO (a,d,g) for 1 h, or 14 μ M AG1478 (b,e,h) for 1 h, or 10 μ M Nocodazole (c) for 1 h, or 500 nM Bafilomycin A1 (f) for 1 h, or 50 mM DOG+0.05 %NaN₃ (i) for 30 min. Cells were stained with an antibody against tubulin (a,b,c), or β -COP (g,h,i), or an dye lysotracker (d,e,f). (j) H4 cells were treated with DMSO, AG1478, BFA and DOG/NaN₃ for 30 min and the levels of ATP were determined with Sigma ATP Bioluminescent Assay kit. Bar, 10 μ m.



Supplemental Fig. 2 The effect of AG1478 or BFA on cell viability. H4 cells were treated with DMSO, 5 μ M BFA, 14 μ M AG1478 alone or with z-VAD together as indicated for 24 h or 48 h, performed by MTT assay. Numbers represent viability normalized to that of 0.1% DMSO treated cells.



Supplemental Fig. 3 The example processed images for analysis by CellProfiler.



Supplemental Table 1. The effect of AG1478 or BFA on Golgi in cell lines

	cell lines	AG1478 (28 μ M \approx 10 μ g/ml)	BFA (5 μ M)
Human	H4	√	√
	HeLa	√	√
	HepG2	√	√
	A549	√	√
	293T	√	√
	Hs 578Bst	√	√
Mouse	NIH 3T3	×	√
	MEFs	×	√
	B16	×	√
	P19	×	√
	L929	×	√
Rat	NRK	×	√
	Rat2	×	√
	Rat1	×	√
	PC12	×	√
Kangaroo rat	PtK1	×	×
Dog	MDCK	×	×

("√" represents compounds that have a dispersal effect on Golgi in cell lines; "×" represents compounds that have no dispersal effect on Golgi in cell lines;)